Rapid Communications

Supersolid behavior of a dipolar Bose-Einstein condensate confined in a tube

Santo Maria Roccuzzo[1] and Francesco Ancilotto[2,3]

[1]*INO-CNR BEC Center and Dipartimento di Fisica, Università di Trento, 238123 Povo, Italy*

[2]*Dipartimento di Fisica e Astronomia "Galileo Galilei" and CNISM, Università di Padova, Via Marzolo 8, 35122 Padova, Italy*

[3]*CNR-IOM Democritos, via Bonomea, 265-34136 Trieste, Italy*

(Received 2 November 2018; published 2 April 2019)

Motivated by a recent experiment [L. Chomaz *et al.*, Nat. Phys. **14**, 442 (2018)], we perform numerical simulations of a dipolar Bose-Einstein condensate (BEC) in a tubular, periodic confinement at $T = 0$ within density functional theory, where the beyond-mean-field correction to the ground-state energy is included in the local density approximation. We study the excitation spectrum of the system by solving the corresponding Bogoliubov–de Gennes equations. The calculated spectrum shows a roton minimum, and the roton gap decreases by reducing the effective scattering length. As the roton gap disappears, the system spontaneously develops a periodic linear structure formed by denser clusters of atomic dipoles immersed in a dilute superfluid background. This structure shows the hallmarks of a supersolid system, i.e., (i) a finite nonclassical translational inertia along the tube axis and (ii) the appearance of two gapless modes, i.e., a phonon mode associated with density fluctuations and resulting from the translational discrete symmetry of the system, and a Nambu-Goldstone gapless mode corresponding to phase fluctuations, resulting from the spontaneous breaking of the gauge symmetry. A further decrease in the scattering length eventually leads to the formation of a periodic linear array of self-bound droplets.

DOI: 10.1103/PhysRevA.99.041601

Dipolar Bose-Einstein condensates (BECs) have attracted great attention in recent years, since the first experimental realizations of BECs with strongly magnetic atomic gases [1–3]. This interest is motivated by the particular properties of such systems which are characterized by anisotropic and long-range dipole-dipole interactions in addition to short-range contact interactions, resulting in a geometry-dependent stability diagram [4] where the system [which is intrinsically unstable in three dimensions (3D)] becomes stable against collapse if the confinement along the polarization axis is much tighter that the in-plane confinement. The properties of dipolar BECs have been the subject of numerous experimental and theoretical studies, which are extensively reviewed in Refs. [5,6].

Recent experiments [7,8] on the stability of a dipolar BEC of ^{164}Dy trapped in a flat "pancake" trap showed the formation of droplets arranged in an ordered structure, their collapse being prevented by the tight confinement along the short axis. This effect is the equivalent of the Rosensweig instability of classical ferrofluids [9].

Remarkably, recent experiments [10] showed that *self-bound* droplets can be realized in a dipolar Bose gas depending upon the ratio between the strengths of the long-range dipolar attraction and the short-range contact repulsion. These droplets, whose densities are higher by about one order of magnitude than the density of the weakly interacting condensate, are stable even in free space, after the external trapping potential is removed.

The possibility of self-bound dipolar droplets has been explained theoretically in Refs. [11–13], where it has been shown that the binding arises from the interplay between the two-body dipolar interactions and the effects of quantum fluctuations. The latter can be embodied in a beyond-mean-field energy correction [11,14], where a positive shift of the ground-state energy with the Lee-Huang-Yang (LHY) form [15] counteracts the destabilizing effect of the dipole-dipole attraction. The crossover in a dipolar quantum fluid from a dilute BEC to self-bound macrodroplets was studied in Ref. [13], where further evidence was provided that quantum fluctuations indeed stabilize the ultracold gas far beyond the instability threshold imposed by mean-field interactions. The properties of self-bound dipolar quantum droplets have been extensively studied from a computational point of view, both within a mean-field theory approach that takes into account the LHY correction [12,16], and with quantum Monte Carlo simulations [17–19].

In Ref. [20] it has been shown that in a dipolar BEC of ^{166}Er confined in a strongly prolate cigar-shaped trap ("tubular" trap), the reduction of the scattering length leads to the appearance of a roton mode. The excited-state dispersion relation is thus characterized by a roton minimum, similarly to the case of ^{4}He, the roton gap amplitude depending on the relative strengths of short-range and dipolar interactions, as predicted in Refs. [21,22]. This suggests that when the roton gap becomes very small, a dipolar BEC confined in an axially elongated trap orthogonal to the polarization direction may develop a modulated density profile in its ground state. Based on this, it has been suggested [20] that this system may indeed show supersolid behavior.

The existence of a supersolid phase of matter was proposed long ago for ^{4}He [23], but its experimental verification remained elusive [24]. The possibility of forming a solid

structure simultaneously possessing crystalline order and superfluid properties [25] is associated with an excitation spectrum of the liquid phase characterized by a roton minimum at a finite k vector [26], the liquid-to-supersolid transition being triggered by the vanishing of the roton gap. Supersolid phases have been recently predicted for confined condensed spinless bosons in 2D [27] and 3D [28] interacting via a broad class of soft-core repulsive potentials.

Supersolid behavior has been proposed for the stripe phase of a dipolar Bose gas under strong confinement when the polarization axis forms an angle with the tight confinement axis [29–31]. Similar predictions have been made for a dipolar BEC confined in a quasi-2D pancake-shaped trap [32], where possible supersolid behavior is related to the formation of a low-density "halo" of atoms among different droplets in a cluster arrangement when the chemical potential is high enough to let some atom escape from a single droplet. Finally, supersolid behavior has been suggested in a ferrofluid mixture of dipolar BEC under a "pancake" confinement [33], within a mean-field approach.

The only experimental evidence so far of supersolid behavior in cold gases has been reported recently in Ref. [34], where the authors realized an "infinitely stiff" supersolid of ^{87}Rb atoms with the density modulation artificially imposed by external optical lattices. Stable "stripe" modulations have been experimentally observed recently in dipolar quantum gas [31,35]. While no global phase coherence is found in a similar system studied in Ref. [31], a partial phase coherence is suggested in Ref. [35], thus indicating possible supersolid behavior.

We notice that in the systems studied in Refs. [31,32], the condensate → droplet transition results in the formation of finite clusters made of a few stripes (i.e., a very elongated droplet in the polarization direction). In both of the above two studies many local minima of the total energy are possible, depending upon the number of atoms in the condensate, and these minima are characterized by the different number and arrangement of droplets. One such state appears to be a stationary state with a global coherence that is predicted to be robust against quantum phase fluctuations [32].

We will propose in the following a different geometry, where the condensate-droplet transition occurs in a tubular confinement with periodic boundary conditions, resulting in a density-modulated configuration made by a linear periodic arrangement of equally spaced elongated "droplets" immersed in a halo of low-density superfluid. We will provide here evidence of the supersolid character of such a structure.

In this Rapid Communication, we will use numerical simulations within density functional theory (DFT) at $T = 0$, in the local density approximation (LDA), to study the equilibrium structure and elementary excitations of a dipolar BEC confined in a tube whose axis is orthogonal to the polarization direction, and with periodic boundary conditions along the tube axis.

Within the DFT framework, the total energy of a dipolar BEC of atoms with mass m and magnetic moment $\boldsymbol{\mu}$ is

$$E = \int \left[\frac{\hbar^2}{2m}|\nabla\phi(\mathbf{r})|^2 + V_t(\mathbf{r})|\phi(\mathbf{r})|^2 + \frac{g}{2}|\phi(\mathbf{r})|^4\right]d\mathbf{r} + \frac{1}{2}\int V_{dd}(|\mathbf{r}-\mathbf{r}'|)|\phi(\mathbf{r})|^2|\phi(\mathbf{r}')|^2 d\mathbf{r}\,d\mathbf{r}' + \frac{2}{5}\gamma(\epsilon_{dd})\int|\phi(\mathbf{r})|^5 d\mathbf{r}. \quad (1)$$

Here, $g = \frac{4\pi\hbar^2 a}{m}$, a being the s-wave scattering length, $V_{dd}(\mathbf{r}-\mathbf{r}') = \frac{\mu_0\mu^2}{4\pi}\frac{1-3\cos^2\theta}{|\mathbf{r}-\mathbf{r}'|^3}$ is the dipole-dipole interaction between two identical magnetic dipoles aligned along the z axis (θ being the angle between the vector $\mathbf{r}$ and the polarization direction z), and μ_0 is the permeability of the vacuum. V_t is the trapping potential. The last term is the beyond-mean-field [Lee-Huang-Yang (LHY)] correction [14], where $\gamma(\epsilon_{dd}) = \frac{32}{3\sqrt{\pi}}ga^{\frac{3}{2}}F(\epsilon_{dd})$, $\epsilon_{dd} = \frac{\mu_0\mu^2}{3g}$ being the ratio between the strengths of the dipole-dipole and contact interactions, and $F(\epsilon_{dd}) = \frac{1}{2}\int_0^\pi d\theta\,\sin\theta[1+\epsilon_{dd}(3\cos^2\theta-1)]^{\frac{5}{2}}$. The number density of the dipole system is $n(\mathbf{r}) = |\phi(\mathbf{r})|^2$.

The minimization of the above energy functional leads to the following Euler-Lagrange (EL) equation,

$$H_0\phi(\mathbf{r}) \equiv \left[-\frac{\hbar^2}{2m}\nabla^2 + V_t(\mathbf{r}) + g|\phi(\mathbf{r})|^2 + \gamma(\epsilon_{dd})|\phi(\mathbf{r})|^3 + \int d\mathbf{r}'|\phi(\mathbf{r}')|^2 V_{dd}(\mathbf{r}-\mathbf{r}')\right]\phi(\mathbf{r}) = \mu\phi(\mathbf{r}), \quad (2)$$

and μ is a Lagrange multiplier whose value is determined by the normalization condition $\int|\phi(\mathbf{r})|^2 d\mathbf{r} = N$ (N being the total number of dipoles). Equation (2) is the well-known Gross-Pitaevskii equation [36] with the addition of the LHY correction. In what follows, m is the mass of an ^{166}Er atom. A similar approach has been used, e.g., in Ref. [11] and other papers addressing the effect of beyond-mean-field effects on the dipolar Bose gas. The predictions of the DFT-LHY approach described above have been tested in Ref. [17] against quantum Monte Carlo simulations, showing that the DFT-LHY indeed allows rather accurate predictions.

In the following, we will assume a tubular confinement, i.e., the dipoles are radially confined by a harmonic potential $V_t(\mathbf{r}) = \frac{1}{2}m(\omega_y^2 y^2 + \omega_z^2 z^2)$, in the y-z plane (z is the polarization direction and y is the transverse direction). The harmonic frequencies are fixed to the values $\omega_y = \omega_z = 2\pi(600)$ Hz. This geometry closely matches the experimental setup used in the recent experiments of Refs. [13,20]. Along the third axis, x, the system is not confined, but subject to periodic boundary conditions (PBCs), $\phi(x+L,y,z) = \phi(x,y,z)$, L being the tube length. Note that, due to the presence of PBCs, the system is equivalent to a ring geometry (with a ring radius $R = L/2\pi$), if curvature effects can be neglected (i.e., when R is much larger that the harmonic confinement length in the y-z plane). This allows us to test our prediction in actual experiments, where a ring-shaped trapping potential can be easily realized.

We solve Eq. (2) by propagating in imaginary time its time-dependent counterpart $i\hbar\partial\phi/\partial t = H_0\phi$. In all the simulations we fix the value of the linear density $n_0 = N/L$ and vary the value of the ratio ϵ_{dd} between the dipolar and contact interaction strengths. The total number of atoms is fixed to

$N = 6 \times 10^4$. To compute the spatial derivatives appearing in (2), we used an accurate 13-point finite-difference formula. Density n and wave function ϕ are represented in real space on a three-dimensional spatial mesh with spacing $h = 0.1$ μm. The convolution integral in the potential energy term of Eq. (2) is efficiently evaluated in reciprocal space by using fast Fourier transforms, recalling that the Fourier transform of the dipolar interaction is [5] $\tilde{V}_{\mathbf{k}} = (\mu_0\mu/3)(3\cos^2\alpha - 1)$, where α is the angle between $\mathbf{k}$ and the z axis. We verified that the transverse dimensions of our simulation cell are wide enough to make negligible the effects, on the energy values and density profiles, of the spurious dipole-dipole interaction between periodically repeated images.

In order to study the elementary excitations, we expand the wave function in the Bogoliubov–de Gennes (BdG) form $\Phi(\mathbf{r}, t) = e^{-i\frac{\mu}{\hbar}t}[\phi(\mathbf{r}) + u(\mathbf{r})e^{-i\omega t} - v^*(\mathbf{r})e^{i\omega t}]$, and insert this expansion in Eq. (2). Keeping only terms linear in the amplitudes u and v, one gets the BdG equations for the amplitudes u and v and the excitation energies ϵ, that can be cast in a matrix form as [16]

$$\begin{pmatrix} H_0 - \mu + \hat{X} & -\hat{X}^\dagger \\ \hat{X} & -H_0 + \mu + \hat{X}^\dagger \end{pmatrix} \begin{pmatrix} u \\ v \end{pmatrix} = \epsilon \begin{pmatrix} u \\ v \end{pmatrix}, \quad (3)$$

where H_0 is given in Eq. (2) and the operator $\hat{X}$ is defined by its action on the function f as

$$\hat{X} f(\mathbf{r}) = \phi(\mathbf{r}) \int d\mathbf{r}' [V_{dd}(\mathbf{r} - \mathbf{r}') + g\delta(\mathbf{r} - \mathbf{r}')]\phi^*(\mathbf{r}') f(\mathbf{r}') + \frac{3}{2}\gamma(\epsilon_{dd})|\phi(\mathbf{r})|^3 f(\mathbf{r}). \quad (4)$$

Because of our use of Fourier transforms, which imply that PBCs must be imposed in our calculations, we can expand the wave function ϕ and the complex functions u, v in the Bloch form appropriate to a periodic system. In this way, Eqs. (3) can be solved in reciprocal space allowing us to find $\epsilon_{\mathbf{k}}$ in the right-hand side of Eq. (3) [see Ref. [28] for details about the numerical methods used to solve Eq. (3)].

We first solve the BdG equations to compute the excitation spectrum for a dipole system characterized by a uniform density along the tube axis (x axis). The energies $\epsilon_{\mathbf{k}}$ of the mode along the k_x direction are shown in Fig. 1 (upper panel) for the choice $n_0 = 3.78 \times 10^3$ μm^{-1}, for different values of ϵ_{dd}. Notice that, as ϵ_{dd} is increased (i.e., the scattering length a is decreased), a roton minimum develops in the dispersion relation, eventually vanishing at $\epsilon_{dd} = 1.45$.

This signals a possible density modulation instability that might break the uniform symmetry along the tube axis. In order to verify this, we calculated the equilibrium density profile by solving Eq. (2) for different values of ϵ_{dd}. In Fig. 1 we show the resulting density for two different values of ϵ_{dd}. We plot in Fig. 1 the density $n_y(x, z) = \int n(x, y, z)dy$ integrated along the y axis perpendicular to the polarization direction. One can see that the density remains uniform along the tube for finite values of the roton gap, while it becomes periodically modulated as the roton gap vanishes. The resulting structure in the latter case is shown in the lower panel of Fig. 1. The periodicity of the density profile is fixed by $\lambda = \frac{2\pi}{k_x^c}$, where k_x^c is the critical value of the momentum at which the roton gap vanishes. When the tube length is not commensurate with the roton wavelength, as is the case shown in the figure, the modulation develops at a wavelength most close to it. Such a periodic modulation is maintained well below the transition, as shown in the lowest plot in Fig. 1.

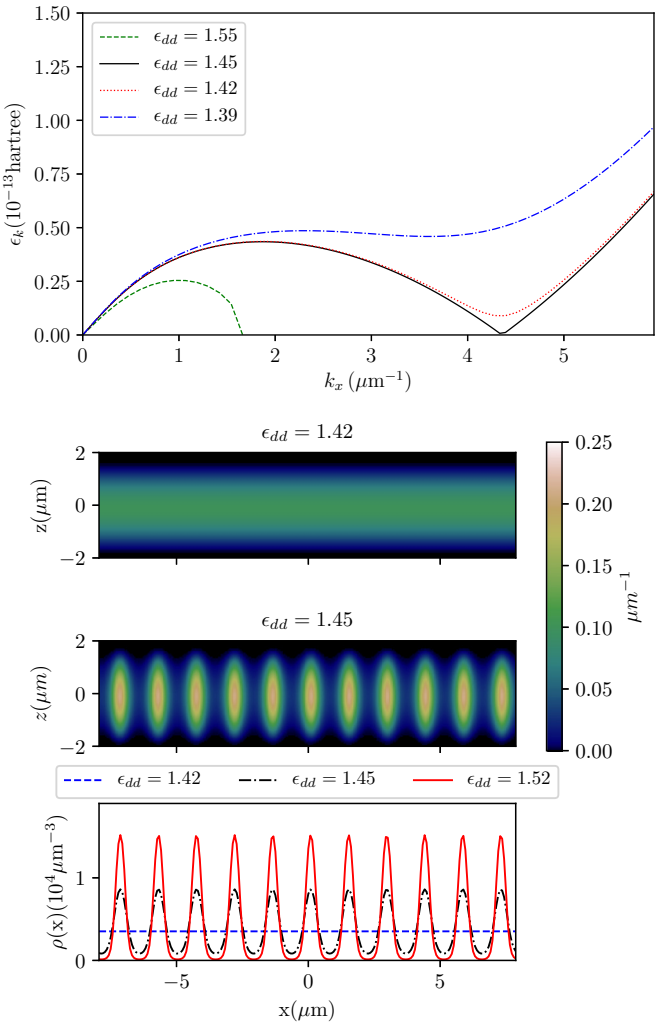

FIG. 1. Upper panel: Dispersion relation of excitations propagating along the tube axis in the homogeneous system. Energies are in atomic units. Lower panel: Integrated density $n_y(x, z)$ just below and at the critical value of ϵ_{dd} where the roton gap vanishes. The total number of atoms is $N = 6 \times 10^4$. The lowest plot shows the density n along the tube axis for different values of ϵ_{dd}.

If we start instead from an initial state modulated with a wavelength different from $2\pi/k_x^c$, we sometimes got trapped, during the minimization procedure, into metastable states characterized by a different number of stripes, with a higher energy than the state shown in Fig. 1. This happens, for instance, with a state having 12 or 9 stripes in the tube (for values of ϵ_{dd} close to the roton instability value $\epsilon_{dd} = 1.45$), instead of the 11 stripes found for the ground state (a 10-stripe solution is found to be unstable towards the lowest-energy 11-stripe structure, i.e., it always evolves towards it during the imaginary-time evolution). The energy differences with respect to the ground state are, however, very small (the 12-stripe state being almost degenerate with the 11-stripe one, with just a 0.1% relative difference, while we find a 1%

relative difference for the 9-stripe case). This implies that during a rapid quench of the interaction the system might indeed get caught into one of these metastable states. The resulting structures, however, still have supersolid properties, being characterized simultaneously by periodic order and a finite nonclassical translational inertia (see the following). Finally, although close to the roton instability our structure is a bona fide ground state, we cannot exclude that for higher values of ϵ_{dd}, the solution we find is a metastable state rather than a ground state.

The periodic structure corresponding to $\epsilon_{dd} = 1.45$ appears to be made of regularly arranged, dense, elongated clusters of dipoles immersed in a background of a very dilute condensate, as shown in the lowest-density plot of Fig. 1. This suggests that the systems, for $\epsilon_{dd} > 1.45$, may display a supersolid character. In order to verify this hypothesis, we have looked for the characteristic hallmarks of supersolid behavior of the modulated structures, i.e., Ref. [37], (i) a finite nonclassical translational inertia and (ii) the appearance, besides the phonon mode associated with the density periodicity, of a gapless "superfluid band" resulting from the spontaneous breaking of global gauge symmetry.

First, we check for the presence of nonclassical translational inertia (NCTI). This is done by solving for stationary states the real-time version of the EL equation (2) in the comoving reference frame with uniform velocity v_x, i.e.,

$$i\hbar\frac{\partial}{\partial t}\phi(\mathbf{r}) = \left(H_0 + i\hbar v_x\frac{\partial}{\partial x}\right)\phi(\mathbf{r}). \tag{5}$$

Following Ref. [37], we define the superfluid fraction f_s as the fraction of particles that remains at rest in the comoving frame,

$$f_s = 1 - \lim_{v_x\to 0}\frac{\langle P_x\rangle}{Nmv_x}, \tag{6}$$

where $\langle P_x\rangle = -i\hbar\int\phi^*\partial\phi/\partial x$ is the expectation value of the momentum and Nmv_x is the total momentum of the system if all the particles were moving (f_s should not be confused with the total superfluid fraction; for instance, in the deep nonlinear regime where self-bound droplets form, as shown in the following, although they are individually superfluid, f_s is zero, meaning that there is no supersolid behavior).

The definition above is the most natural to reveal a global phase coherence in a periodic system such as the one studied here [37]. Other ways of quantifying the tunneling in strongly confined systems made of a cluster of droplets are possible, such as, e.g., approximately treating pairs of droplets as bosonic Josephson junctions [31,32].

We can see from Fig. 2 that, when a modulation in the density profile appears, the superfluid fraction becomes smaller than one, and it decreases as ϵ_{dd} is increased. A small jump at the uniform → modulated transition seems to signal a first-order transition, similarly to what is found in the case of a supersolid transition of soft-core bosons [28].

Another characteristic of supersolid behavior is associated with the presence in the excitation spectrum of the periodically modulated structure shown in Fig. 1, of an extra gapless mode besides the "phonon" modes associated with the periodic density modulations [38]. The excitation spectrum can be calculated by solving the corresponding BdG

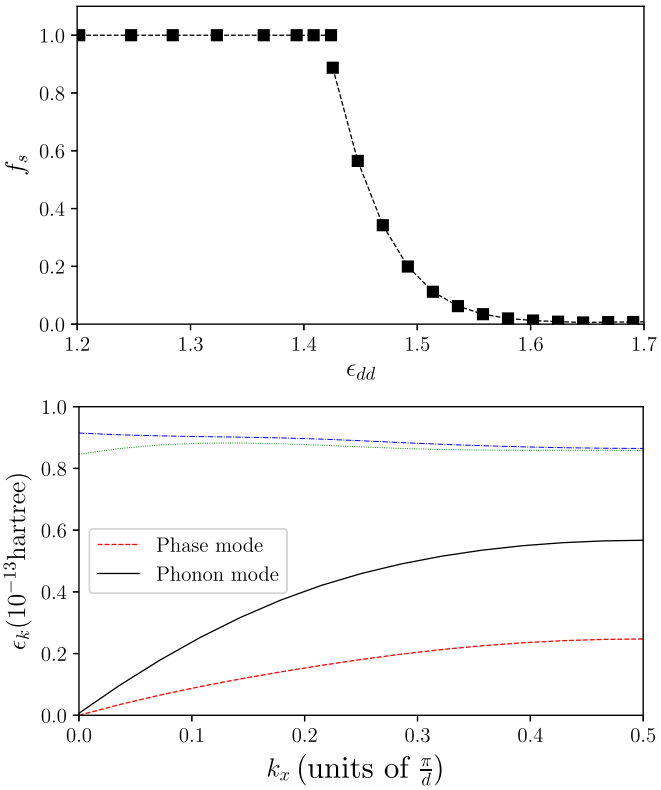

FIG. 2. Upper panel: Superfluid fraction as function of ϵ_{dd}. Lower panel: Excitation spectrum along the tube axis, calculated for $\epsilon_{dd} = 1.45$. The rightmost value of k_x corresponds to the first Brillouin zone boundary along the x axis, i.e., $k_x = \pi/d$, $d = L/11$ being the length of the unit cell containing exactly one droplet in Fig. 1.

equations for modes propagating along the axis of the tube. The result is shown in Fig. 2, for the values $\epsilon_{dd} = 1.45$ and $n_0 = 3.78\times 10^3\ \mu\text{m}^{-1}$, from which one can see the appearance of two gapless modes associated with symmetry breaking. The harder mode is associated with the density response of the system, and it corresponds to the phonon branch. The softer mode is associated instead with the phase response of the system, and it signals the superfluid character of the supersolid (Nambu-Goldstone mode). The correct mode assignment was made by looking at the calculated local density and phase fluctuation modes [28,39], $\Delta\rho_{n\mathbf{k}}(\mathbf{r}) = |u_{n,\mathbf{k}} - v_{n,\mathbf{k}}|^2$ and $\Delta\theta_{n\mathbf{k}}(\mathbf{r}) = |u_{n,\mathbf{k}} + v_{n,\mathbf{k}}|^2$, respectively: The phonon mode is mainly characterized by density modulations, whereas the superfluid mode is characterized mainly by modulations in the phase. As ϵ_{dd} increases, the system is entering the regime of self-bound droplets (as discussed below), and as a result the Goldstone phase mode become softer and softer, until it completely disappears. In this regime the droplets are disconnected from one another and the superfluid fraction associated with the nonclassical inertia goes to zero, while the individual droplets are still superfluid.

From Fig. 2 (upper panel) it appears that as ϵ_{dd} increases, the superfluid fraction tends to zero. When this happens, the atomic clusters shown in the lowest panel of Fig. 1 begin to merge, forming denser isolated droplets, while the calculated energy per particle becomes negative, as shown

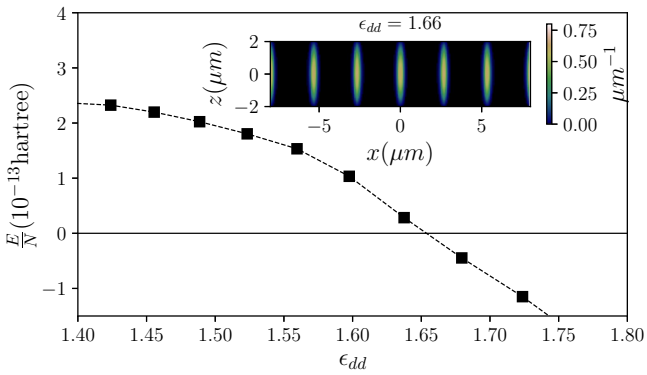

FIG. 3. Energy per particle (in atomic units) as a function of ϵ_{dd}. The inset shows the array of self-bound droplets.

in Fig. 3. This happens at $\epsilon_{dd} \sim 1.66$. Above this value, the density profile of the system takes the form of an (ordered) one-dimensional lattice of *self-bound* quantum droplets (each containing $N \sim 10^4$ atoms), while the supersolid behavior is completely suppressed, as shown by the disappearance of the Nambu-Goldstone mode from the calculated excitation spectrum.

We notice at this point that we obtained similar results with different choices for the system density and tube length. However, there is no special choice for such parameters which will give supersolid properties. Rather, for a given density, tube length, and radial confinement, there is always a range of coupling strengths where the system shows supersolid behavior: A different choice of parameters will only shift the condensate-supersolid transitions towards different values of the coupling strength, but the relevant physics will not be affected. (The density must, however, be large enough for the system to develop the expected modulation.) We notice, however, that for very long tubes (much longer than the ones investigated here) quantum phase fluctuations may destroy the phase relationship between distant droplets.

Preliminary calculations show that the supersolid character of the system described here is robust against weak perturbations of the external potential. In particular, small periodic modulations of the trapping potential do not destroy the supersolid behavior [40].

In conclusion, we have shown, by means of numerical simulations based on the DFT-LHY approach, that in a dipolar BEC confined in a tube at $T = 0$, the softening of the roton mode, caused by a decrease in the scattering length, leads to the formation of a modulated, periodic structure, in which denser clusters of dipoles are immersed in a very dilute superfluid background. This system shows the hallmarks of supersolid behavior, i.e., a finite, nonclassical translational inertia, and a Goldstone "superfluid" mode in the excitation spectrum in addition to the phonon mode associated with density periodicity. The supersolid behavior is suppressed when the system, by further decreasing the scattering length, enters into a regime in which the dipole clusters turn into an ordered array of self-bound quantum droplets. The tubular confinement is more convenient from an experimental point of view than a 2D confinement because it likely reduces the number of possible metastable states with comparable energies.

The phase coherence of the supersolid phase described here could be experimentally detected in a dipolar condensate confined in a ring trap where, after having tuned the scattering length across the threshold value required for the supersolid formation, the trapping potential is switched off, allowing the system to expand freely. By doing subsequent absorption imaging, one could detect the presence of interference maxima associated with phase coherence [34].

Note added. Recently, a joint experimental-theoretical paper appeared [41] showing that a ground-state, coherent linear array of quantum "droplets" can be realized where, in addition to periodic density modulations, a robust phase coherence across the system is maintained, similarly to what we predicted here.

We thank A. Recati, L. Salasnich, and S. Stringari for useful exchanges. S.M.R. acknowledges funding from Provincia Autonoma di Trento.

[1] A. Griesmaier, J. Werner, S. Hensler, J. Stuhler, and T. Pfau, Phys. Rev. Lett. **94**, 160401 (2005).
[2] M. Lu, N. Q. Burdick, S. H. Youn, and B. L. Lev, Phys. Rev. Lett. **107**, 190401 (2011).
[3] K. Aikawa, A. Frisch, M. Mark, S. Baier, A. Rietzler, R. Grimm, and F. Ferlaino, Phys. Rev. Lett. **108**, 210401 (2012).
[4] T. Koch, T. Lahaye, J. Metz, B. Fröhlich, A. Griesmaier, and T. Pfau, Nat. Phys. **4**, 218 (2008).
[5] T. Lahaye, C. Menotti, L. Santos, M. Lewenstein, and T. Pfau, Rep. Prog. Phys. **72**, 126401 (2009).
[6] M. A. Baranov, M. Dalmonte, G. Pupillo, and P. Zoller, Chem. Rev. **112**, 5012 (2012).
[7] H. Kadau, M. Schmitt, M. Wenzel, C. Wink, T. Maier, I. Ferrier-Barbut, and T. Pfau, Nature (London) **530**, 194 (2016).
[8] I. Ferrier-Barbut, M. Wenzel, M. Schmitt, F. Böttcher, and T. Pfau, Phys. Rev. A **97**, 011604(R) (2018).
[9] M. D. Cowley and R. E. Rosensweig, J. Fluid Mech. **30**, 671 (1967).
[10] M. Schmitt, M. Wenzel, F. Bottcher, I. Ferrier-Barbut, and T. Pfau, Nature (London) **539**, 259 (2016).
[11] F. Wächtler and L. Santos, Phys. Rev. A **93**, 061603(R) (2016).
[12] D. Baillie, R. M. Wilson, R. N. Bisset, and P. B. Blakie, Phys. Rev. A **94**, 021602(R) (2016).
[13] L. Chomaz, S. Baier, D. Petter, M. J. Mark, F. Wachtler, L. Santos, and F. Ferlaino, Phys. Rev. X **6**, 041039 (2016).
[14] A. R. P. Lima and A. Pelster, Phys. Rev. A **84**, 041604(R) (2011).
[15] K. Huang and C. N. Yang, Phys. Rev. **105**, 767 (1957).
[16] D. Baillie, R. M. Wilson, and P. B. Blakie, Phys. Rev. Lett. **119**, 255302 (2017).
[17] H. Saito, J. Phys. Soc. Jpn. **85**, 053001 (2016).
[18] A. Macia, J. Sánchez-Baena, J. Boronat, and F. Mazzanti, Phys. Rev. Lett. **117**, 205301 (2016).

[19] F. Cinti, A. Cappellaro, L. Salasnich, and T. Macrì, Phys. Rev. Lett. **119**, 215302 (2017).
[20] L. Chomaz, R. M. W. van Bijnen, D. Petter, G. Faraoni, S. Baier, J. H. Becher, M. J. Mark, F. Wächtler, L. Santos, and F. Ferlaino, Nat. Phys. **14**, 442 (2018).
[21] L. Santos, G. V. Shlyapnikov, and M. Lewenstein, Phys. Rev. Lett. **90**, 250403 (2003).
[22] D. H. J. O'Dell, S. Giovanazzi, and G. Kurizki, Phys. Rev. Lett. **90**, 110402 (2003).
[23] E. P. Gross, Phys. Rev. **106**, 161 (1957).
[24] D. Y. Kim and M. H. W. Chan, Phys. Rev. Lett. **109**, 155301 (2012).
[25] M. Boninsegni and N. V. Prokof'ev, Rev. Mod. Phys. **84**, 759 (2012).
[26] D. A. Kirzhnits and Yu. A. Nepomnyashchiĭ, Sov. Phys. JETP **32**, 1191 (1971).
[27] F. Cinti, P. Jain, M. Boninsegni, A. Micheli, P. Zoller, and G. Pupillo, Phys. Rev. Lett. **105**, 135301 (2010).
[28] F. Ancilotto, M. Rossi, and F. Toigo, Phys. Rev. A **88**, 033618 (2013).
[29] R. Bombin, J. Boronat, and F. Mazzanti, Phys. Rev. Lett. **119**, 250402 (2017).
[30] F. Cinti and M. Boninsegni, Phys. Rev. A **96**, 013627 (2017).
[31] M. Wenzel, F. Bottcher, T. Langen, I. Ferrier-Barbut, and T. Pfau, Phys. Rev. A **96**, 053630 (2017).
[32] D. Baillie and P. B. Blakie, Phys. Rev. Lett. **121**, 195301 (2018).
[33] H. Saito, Y. Kawaguchi, and M. Ueda, Phys. Rev. Lett. **102**, 230403 (2009)
[34] J. Leonard, A. Morales, P. Zupancic, T. Esslinger, and T. Donner, Nature (London) **543**, 87 (2017).
[35] L. Tanzi, El. Lucioni, F. Famà, J. Catani, A. Fioretti, C. Gabbanini, and G. Modugno, arXiv:1811.02613.
[36] L. P. Pitaevskii, Sov. Phys. JETP **13**, 451 (1961); E. P. Gross, Nuovo Cimento **20**, 454 (1961).
[37] Y. Pomeau and S. Rica, Phys. Rev. Lett. **72**, 2426 (1994); N. Sepulveda, C. Josserand, and S. Rica, Eur. Phys. J. B **78**, 439 (2010).
[38] S. Saccani, S. Moroni, and M. Boninsegni, Phys. Rev. Lett. **108**, 175301 (2012).
[39] T. Macrì, F. Maucher, F. Cinti, and T. Pohl, Phys. Rev. A **87**, 061602(R) (2013).
[40] S. Roccuzzo, A. Recati, and S. Stringari (unpublished).
[41] F. Bottcher *et al.*, Phys. Rev. X **9**, 011051 (2019).